



Original Article

Study of effect of tin on the electrochemical properties of cycled PbSn alloys of lead-acid battery

Toufik Dilmi^{a,b*}, Abdehamid Guelil^{b,c}, Achour Dakhouché^b

^aDepartment of Physics, University Mira Abderahman, Bejaia, Algeria

^bInorganic Materials Laboratory, Department of Chemistry, Faculty of Sciences, Mohamed Boudiaf University, M'sila, Algeria

^cDepartment of natural sciences and life sciences matter sciences, Faculty of exact sciences, Mohamed Khaider University, Biskra, Algeria

ARTICLE INFO

Article history:

Received 07 November 2020

Revised 15 December 2020

Accepted 01 January 2021

Keywords:

alloy;
corrosion;
semiconductor;
acid battery;
Thickness.

ABSTRACT

Tin has a beneficial effect on the electrochemical properties of the corrosion film formed on PbSn grids by reducing its resistivity mainly on cycling of the battery. Binary alloys with different tin contents were subjected to several charge-discharge cycles between and vs. Electrode in solution at. The electrochemical properties of alloys in sulfuric acid solution were studied by Cyclic Voltammetry, Linear Voltammetry and Chronpotentiometry. The compositions of the corrosion layer obtained at different numbers of cycles were determined by DRX. We were found that reduces the thickness and favorites a more conductive and dense layer between the grid and the positive active mass.

© 2021 Faculty of Technology, University of Echahid Hamma Lakhdar. All rights reserved

1. Introduction

The addition of tin in the grid of valve regulated lead acid battery was as an attempt to illuminate the semiconductive layer constituted mainly of and between the collector and the positive active mass [1,2].

The introduction of tin as an alloy with lead dates back to the invention of the lead-acid battery by Planté in order to support the improvement of the mechanical characteristics of the plates. During the oxidation of PbSn alloys, tin is detached from the anode and deposited on the negative plate. It then decreases the hydrogen release overvoltage which increases the decomposition of water. The accumulator must always be under maintenance. In order to free this accumulator from this maintenance (addition of water), it was necessary to replace the tin by calcium which has good mechanical characteristics similar to those of tin. This replacement of tin does not have the desired results regarding corrosion resistance. The PbCa sulphur alloys of the so-called "PCL = premature capacity lost" or the (early capacity loss) due to the formation of a barrier layer of Sulphate and α -PbO which increase the resistance of the

layer between the collector and the active mass. This layer changes during the service of the accumulator isolating a very large quantity of the active mass and thus the lead accumulator is taken out of service. To remedy this phenomenon, different elements have been tested by which tin, which has given good results as a depassivation element, has been used.

It is in this contest that we have tried to contribute to understand first of all the phenomenon itself on tin-free electrodes and after addition of tin to lead. According to [3-11], PbSn and PbSn(Ca) alloys have a beneficial effect on reducing water decomposition.

Many new grid materials have been investigated in recent years to eliminate the disadvantages of PbSb and PbCa alloys on the performance of lead batteries containing different elements such as Ag, Al, Bi, La, Ce and Li [12-17].

This work aims to provide an explanation of the effect of tin on the electrochemical properties of cycled PbSn alloys of lead acid battery. Using different techniques.

* Corresponding author. Tel.: +21365553494

E-mail address: dilmi2826@gmail.com

Peer review under responsibility of University of Echahid Hamma Lakhdar. © 2021 University of Echahid Hamma Lakhdar. All rights reserved.

<http://dx.doi.org/10.5281/zenodo.4408710>

2. Materials and Methods

2.1. Material

The elaboration of the materials was carried out by fusion of pure metals (Pb and Sn) in a porcelain crucible. The melting was carried out in an electric resistance furnace. At

2.2. The electrochemical cell

The electrochemical experiments are performed with an AUTOLAB PGSTAT302N potentiostat/galvanostat controlled by a computer that records the data with NOVA 2.1 software, allowing the exploitation of the results of this study. The cell and the electrodes are connected directly to the device. The electrochemical cell is made of glass with

a temperature of 328°C, the bath formed was stirred slightly with a stainless steel spoon in order to achieve maximum homogeneity of the material.

The alloy in the liquid state is cast in a parallelepipedal metal mould with dimensions (75 x 25 x 190) mm. The ingot obtained is sawn into several pieces to be used as samples for different analyses.

a hole on one side (for the working electrode) and a glass cover with 02 holes allowing the passage of the electrodes (auxiliary and reference). This cell has a capacity of 200 ml containing the electrolyte in which the three electrodes used are immersed: working electrode, auxiliary electrode and reference electrode as shown in Fig. 1.

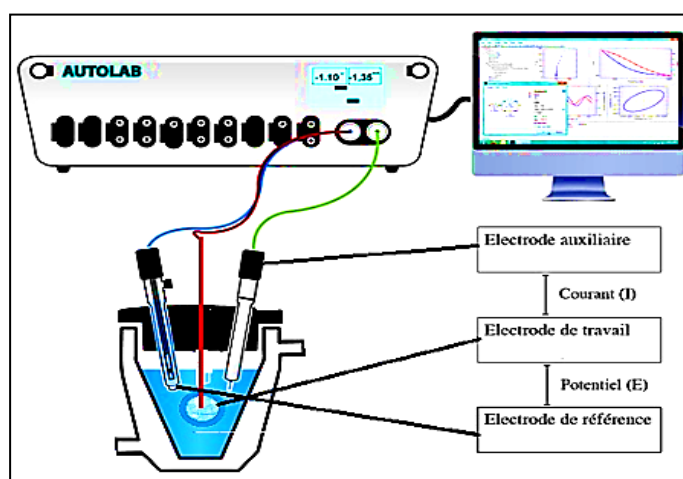


Fig. 1. Schematic representation of the experimental setup

Lead alloys require special care for metallographic analysis because they are very soft and very ductile. Forced polishing could cause deep structural transformations. This is why the entire polishing protocol is done manually. The specimens are prepared by mechanical polishing using an abrasive paper with a magnification of: (1000, 1200 and 2000).

After polishing, the specimens are thoroughly degreased and cleaned using acetone and then washed with distilled water. The electrochemical tests that have been adopted, aim to know the behavior of the alloys in a sulfuric medium (H_2SO_4) at 0.5M, which is the electrolyte used in the manufacture of "batteries" called lead-acid batteries and acid (Lead Acid Batteries) intended for starting vehicles.

The reference electrode used is the mercury sulphate electrode. The electrochemical tests were carried out using an AUTOLAB PGSTAT 302N Potentiostat connected to a microcomputer equipped with computer software used to transform the electrical signals from the electrochemical cell into numerical and graphical data interpreting the electrochemical behaviour of the studied alloys in a sulphuric medium.

2.3. The electrodes used are:

-The reference electrode is a mercury sulphate electrode filled with a saturated potassium sulphate solution, $Hg/Hg_2SO_4/K_2SO_4$.

-The auxiliary electrode is a pure lead electrode with a larger surface area than the working electrode, which ensures the passage of current through the electrical circuit and its measurement.

-The working electrode: we have formed pellets with a diameter of 1 cm and a thickness of 0.5 cm.

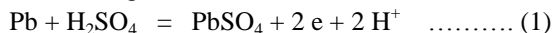
3. Results and Discussion

3.1. Potentiodynamic measurements.

3.1.1. Cyclic Voltammetry

Before any potentiodynamic experiment, the potential of the working electrode is maintained at the hydrogen release potential for 20 minutes in order to reduce any impurities that may exist on the surface. The measurements were carried out using an AUTOLAB PGSTAT302N potentiostat/galvanostat controlled by NOVA 2.1 software, allowing the acquisition and the exploitation of the

obtained results. The ramp is made to scan the potential of the working electrode between -1.2V and 0.7 V with respect to the reference electrode Hg/Hg₂SO₄/K₂SO₄ saturated with a scanning speed of 10 mV/s. A total of 40 relative to the oxidation of Pb to PbSO₄ around -860 mV for the following reaction:



At this moment the electrode is covered with a layer of PbSO₄ and the oxidation current is rapidly decreased (diffusion-controlled kinetics). The cutting of the PbSO₄ crystals is done in such a way as to block any exit when the SO₄²⁻ ions arrive at the surface of the substrate and the electrode is passivated. By increasing the potential a small peak towards -442 mV is noted (A2) corresponding to the oxidation of Pb into α-PbO. This is explained by different

charge-discharge cycles were performed for each alloy. A cycle starting from the hydrogen evolution potential (-1.2V) is eluted on Fig. 2. We notice that when the potential increases anodically, we obtain a noted peak (A1) researchers as being the result of the reaction of Pb²⁺ and the O²⁻ ion which is able to cross the PbSO₄ dense layer because of its small volume compared to that of SO₄²⁻ which has a larger atomic radius than that of the pores left by the PbSO₄ crystals. The passivation domain will continue after this last peak. In the cathode scan after the arrival at 700 mV, we notice a small peak of reduction of PbO to Pb around -900 mV noted (C1). More cathodically, we obtain another cathodic peak of reduction of PbSO₄ to Pb around -981 mV noted (C2) Fig. 2.

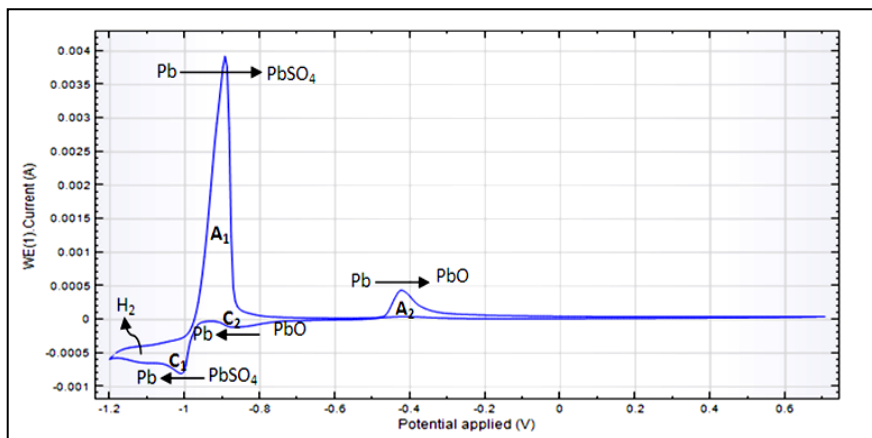


Fig. 2. Different pairs in the potential range from -1.2 to 0.7 V

3.1.2. Linear Voltammetry

Linear Voltammetry is also carried out by scanning the potential of the working electrode between -1.2V and 0.7 V with respect to the reference electrode Hg/Hg₂SO₄/K₂SO₄ saturated with a scanning rate of 10 mV/s in sulphuric acid at 0.5 M at 25°C. The results obtained for the current and corrosion potential at the 10th

and 40th cycle were recorded. A typical voltammogram is shown in Fig. 3. On this voltammogram we observe a peak of oxidation of Pb to PbSO₄. A lead passivation step is then obtained. At this stage the entire surface of the alloy is covered with α -PbO under a layer of lead sulphate. In the area of PbO formation, the appearance of a small peak around 440 mV corresponds to the oxidation of Pb to PbO.

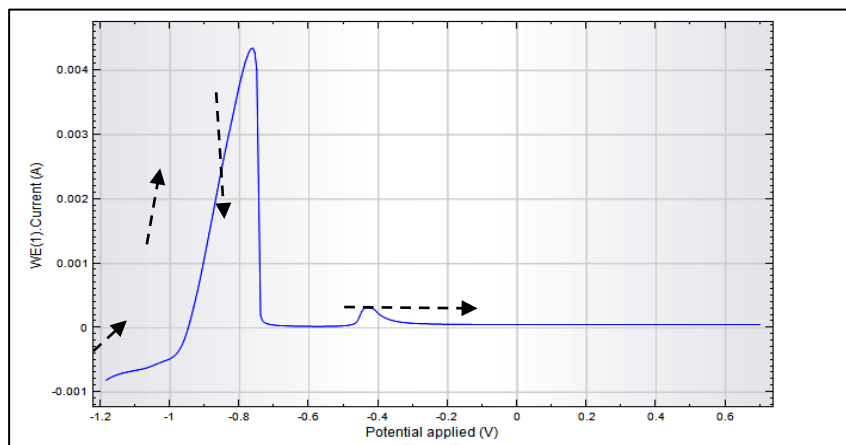


Fig. 3. Example of a linear voltammogram

3.1.3. Tafel curves

The superposition of the Tafel curves of the Pb, Pb -0,2 wt.%Sn and Pb-2 wt.%Sn electrodes are given in Fig. 4.

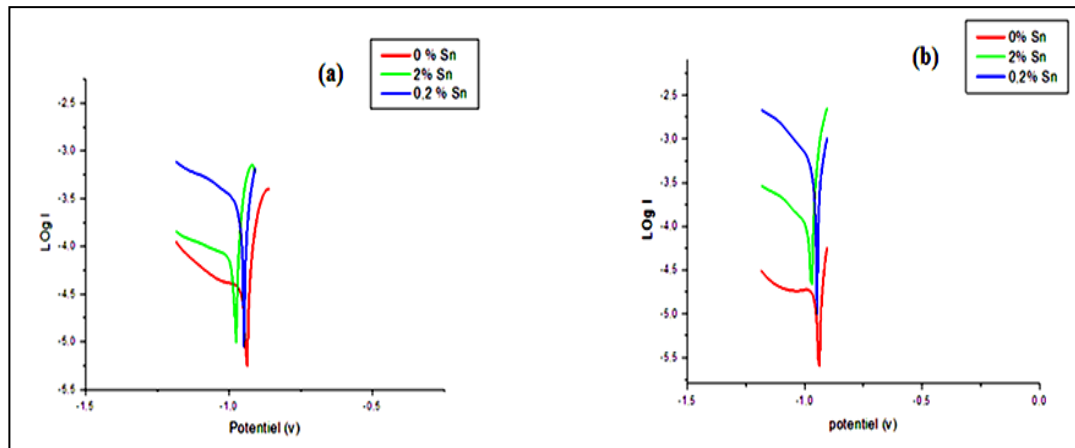


Fig. 4 .Tafel plots: (a) 10 cycles;(b) 40 cycles

The data collected from these Tafel curves are shown in Table 1.

Table 1. Results of I_{corr} and R_p of the different alloys at different cycles according to the Tafel plots.

| N° of cycles | Pb | | | Pb -0,2 wt.%Sn | | | Pb -2 wt.%Sn | | |
|--------------|-----------------------|-----------------|--------------------|-----------------------|-----------------|--------------------|-----------------------|-----------------|--------------------|
| | I_{corr} (μ A) | E_{corr} (mv) | R_p (Ω) | I_{corr} (μ A) | E_{corr} (mv) | R_p (Ω) | I_{corr} (μ A) | E_{corr} (mv) | R_p (Ω) |
| 10 | 19 | -937.59 | 498.97 | 34.27 | -969.82 | 221.81 | 107.1 | -943.28 | 103.4 |
| 40 | 7.063 | -940.65 | 1419.8 | 15.35 | -971.87 | 160.28 | 106.1 | -943.82 | 69 |

To better examine the influence of tin on the corrosion layer resistance of PbSn alloys, we have reported the results obtained from the corrosion current density as a function of number of cycles for the three samples studied on the histogram Fig. 5.

We clearly see that the corrosion current decreases with cycling. This is due to the growth of the corrosion layer consisting mainly of the mixture of $PbSO_4$, α -PbO for Pb

and $PbSO_4$ electrodes, α -PbO and some tin oxides for Pb-0.2 wt.%Sn and Pb-2 wt.%Sn alloys. On the other hand, for a well-defined number of cycles, the corrosion current increases by increasing the tin content within the alloy from 0 to 2%. Tin increases corrosion resistance as the number of cycles increases. In other words, tin decreases the polarization resistance of PbSn alloys.

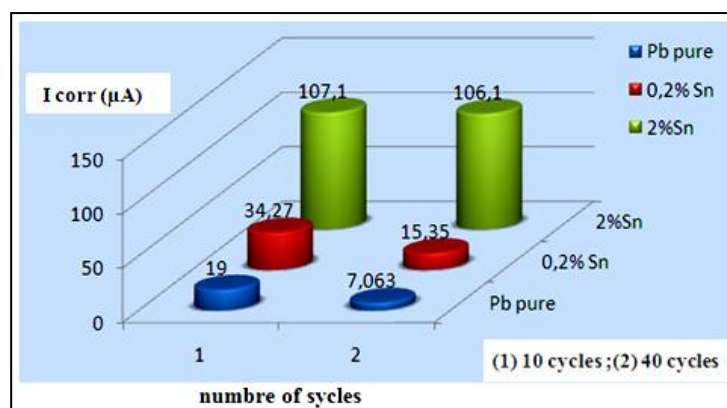


Fig. 5. Histogram of the evolution of corrosion current as a function of number of cycles at different alloys

3.1.4. Evolution of corrosion potential.

The exploitation of the data in Table 1 allowed us to plot the evolution of corrosion potential as a function of the number of cycles for the three electrodes studied.

It is clear that the potential of Pb-0.2 wt.%Sn and Pb-2 wt.%Sn alloys are more negative than that of pure lead. This is explained by the fact that the potential of Sn²⁺/Sn is less noble than that of lead. Tin during its crystallization in the grain boundaries forms an Sn-rich phase. As the grain boundaries have a high energy content, it is at this surface home of the alloy that inter-granular corrosion will start. For the Pb-0.2 wt.%Sn alloy, the amount of Pb-0.2 wt.%Sn is not likely to change the corrosion potential. It should be noted that for the Pb-0.2 wt.%Sn alloy, corrosion occurs at a more cathodic potential than that of Pb-2 wt.%Sn.

3.1.5. Chronopotentiometry

To measure the thickness of the lead monoxide layer,

we used the electrochemical method of chronopotentiometry. It consists in reducing the monoxide layer galvanostatically with a current of -1.5 μA from 700 mV to the transition potential indicating the total reduction of PbO. The thickness is calculated at the 10th and 40th. By Faraday's law:

$$e = \frac{I * t * M}{n * F * S * \rho} \dots\dots\dots (2)$$

With :

- e : the thickness of the layer (μm)
- I : the impressed current (A)
- t : discharge time (s)
- M: the molar mass of PbO (224 g/mol)
- N : number of electrons exchanged
- F: the Faraday (c)
- S: the electrode area (Cm²)
- ρ : PbO density (g/ Cm³)

From these curves we have drawn the transition time for each electrode. The results are grouped in [table 2](#).

Table 2. Discharge time results by chronopotentiometric method

| Pb | | Pb -0,2 wt.%Sn | | Pb -2 wt.%Sn | | |
|--------------|----------|----------------|----------|---------------|----------|---------------|
| N° of cycles | Time (s) | thickness(μm) | Time (s) | thickness(μm) | Time (s) | thickness(μm) |
| 10 | 612 | 14,86 | 558 | 13,56 | 466 | 11,33 |
| 40 | 699 | 17 | 627 | 15,24 | 528 | 12,84 |

We see that as the number of cycles increases, the thickness increases for all electrodes.

We can clearly see that by increasing the tin content in the alloy, the thickness decreases. This is consistent with the literature. The tin thins the lead monoxide layer and thus increases its conductivity.

3.2. Characterization by DRX

The DRX spectra of the 10.40 and 100 cycled samples were performed by Bruker D4 diffractometer using copper as cathode (Cu Kα=1.54 Å) at a voltage of 40 KV from 10 to 60 2θ with a

rotation speed of 0.2 degree/second.

The diffractograms of the Pb, Pb-0.2% Sn and Pb-2% Sn samples are shown in Fig. 6 and Fig. 7. We have taken into consideration that the specific lines of PbSO₄ and α-PbO.

Table 3 summarizes the results obtained from these diffractograms.

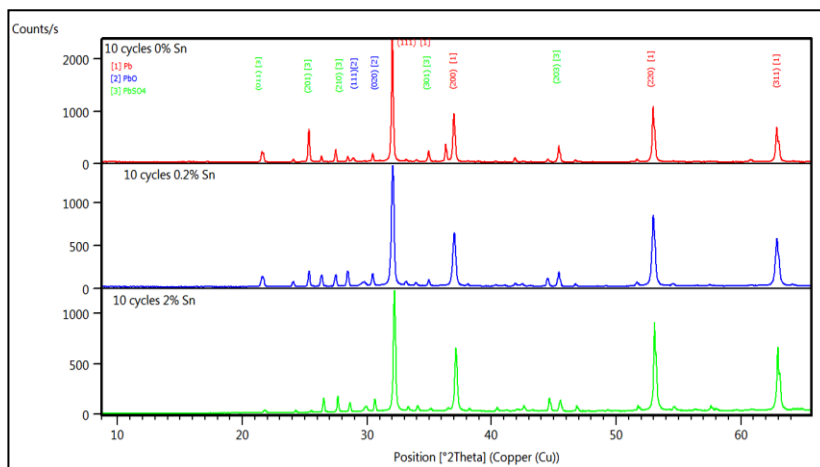


Fig. 6. Diffractogram of sample at 10th cycles of different alloys

References

- [1] R. D. Prengaman, "Challenges from corrosion-resistant grid alloys in lead acid battery manufacturing", *Journal of power sources*, vol. 95, no.1-2, pp.224-233, 2001.
- [2] R. D. Prengaman, "New low-antimony alloy for straps and cycling service in lead–acid batteries", *Journal of power sources*, vol. 158, no. 2, pp. 1110-1116, 2006.
- [3] K. R. Bullock and D. Pavlov, "Advances in lead-acid batteries". In *Proc.-Electrochem. Soc.(United States)*, Johnson Controls Inc., Milwaukee, WI, Vol. 84,1984.
- [4] M. D.Achtermann and M. E. Greenlee, "Application of wrought lead-calcium batteries in Europe", *Journal of Power sources*, vol. 33, no. 1-4, pp. 87-92, 1991.
- [5] G. S. Al-Ganainy, M. T. Mostafa and F. Abd El-Salam, "Quenching media and temperature dependence of structural and stress–strain characteristics of deformed Pb-2 at% Sb alloy during transformation", *Physica B: Condensed Matter*, vol. 348, no. 1-4, pp. 242-248, 2004.
- [6] B. Rezaei and S. Damiri, "Effect of solidification temperature of lead alloy grids on the electrochemical behavior of lead-acid battery", *Journal of Solid State Electrochemistry*, vol. 9, no. 8, pp. 590-594, 2005.
- [7] M. Shiota, T. Kameda, K. Matsui, N. Hirai and T. Tanaka, "Electrochemical properties of lead dioxides formed on various lead alloy substrates". *Journal of power sources*, vol.144, no. 2, pp. 358-364, 2005.
- [8] T. Hirasawa, K. Sasaki, M. Taguchi and H. Kaneko, "Electrochemical characteristics of Pb–Sb alloys in sulfuric acid solutions", *Journal of power sources*, vol. 85, no.1, pp. 44-48, 2000.
- [9] C. S. Lakshmi, J. E.Manders and D. M. Rice, "Structure and properties of lead–calcium–tin alloys for battery grids". *Journal of power sources*, vol. 73, no.1, pp. 23-29, 1998.
- [10] W. R. Osório, C. S. Aoki and A. Garcia, "Hot corrosion resistance of a Pb–Sb alloy for lead acid battery grids". *Journal of power sources*, vol.185, no. 2, pp. 1471-1477, 2008.
- [11] W. R. Osório, C. S.Aoki and A.Garcia, "Effects of microstructural arrangement on hot corrosion resistance of a Pb–Sb alloy for battery grids". In *Materials Science Forum*, vol. 595, pp. 851-859, 2008.
- [12] T. Hirasawa, K. Sasaki, M. Taguchi, H. Kaneko, "Electrochemical characteristics of Pb–Sb alloys in sulfuric acid solutions", *J Power Sources*, vol. 85, pp. 44-48,2000.
- [13] Y.B. Zhou, C.X. Yang, W.F. Zhou, H.T. Liu, " Comparison of Pb–Sm–Sn and Pb–Ca–Sn alloys for the positive grids in a lead acid battery", *J Alloys Compd*, vol. 365, pp. 108-111, 2004.
- [14] A. Maître, G. Bourguignon, J.M. Fiorani, J. Ghanbaja, J. Steinmetz, "Precipitation hardening in Pb–0.08wt.%Ca–x%Sn alloys—the role of the pre-ageing", *Mater Sci Eng A*, vol. 358, pp. 233–242, 2003.
- [15] H. Liu, C. Yang, H. Liang, J. Yang, W. Zhou, "The mechanisms for the growth of the anodic Pb(II) oxides films formed on Pb–Sb and Pb–Sn alloys in sulfuric acid solution", *J Power Sources*, vol. 103, pp. 173–179, 2002.
- [16] D. Slavkov, B.S. Haran, B.N. Popov, F. Fleming, " Effect of Sn and Ca doping on the corrosion of Pb anodes in lead acid batteries", *J Power Sources*, vol. 112, pp. 199–208, 2002.
- [17] J.Z. Liang, H.Y. Chen, M.C. Tang, Y.M. Wu, G.M. Xiao, H.W. Zhou, W.S. Li, X. Jiang, "Properties and application of lead–calcium–tin–aluminium–bismuth alloys for positive grids", *J Power Sources*, vol. 158, pp. 908–913, 2006.

Recommended Citation

Toufik, D., Abdehamid, G., Achou, r D., (2021). Study of effect of tin on the electrochemical properties of cycled PbSn alloys of lead-acid battery. *Algerian Journal of Chemical Engineering*, 01, 01-07. <http://dx.doi.org/10.5281/zenodo.4408710>



This work is licensed under a [Creative Commons Attribution-NonCommercial 4.0 International License](https://creativecommons.org/licenses/by-nc/4.0/)